Evaluation of a Linear Mixing Model to Retrieve Soil and Vegetation Temperatures of Land Targets

Evaluation of a Linear Mixing Model to Retrieve Soil and Vegetation Temperatures of Land Targets

Jinxin YANG [1], Li JIA [1,2*], Yaokui CUI [1], Jie ZHOU [1], Massimo MENENTI [3,1]

[1] State Key Laboratory of Remote Sensing Science, Institute of Remote Sensing and Digital Earth, Chinese Academy of Sciences. Beijing 100101, China

[2] Alterra, Wageningen University and Research Centre, Wageningen, The Netherlands

[3] Delft University of Technology, Delft, the Netherlands

li.jia@wur.nl

Abstract. A simple linear mixing model of heterogeneous soil-vegetation system and retrieval of component temperatures from directional remote sensing measurements by inverting this model is evaluated in this paper using observations by a thermal camera. The thermal camera was used to obtain multi-angular TIR (Thermal Infra-Red) images over vegetable and orchard canopies. A whole thermal camera image was treated as a pixel of a satellite image to evaluate the model with the two-component system, i.e. soil and vegetation. The evaluation included two parts: evaluation of the linear mixing model and evaluation of the inversion of the model to retrieve component temperatures. For evaluation of the linear mixing model, the RMSE is 0.2 K between the observed and modelled brightness temperatures, which indicates that the linear mixing model works well under most conditions. For evaluation of the model inversion, the RMSE between the model retrieved and the observed vegetation temperatures is 1.6K, correspondingly, the RMSE between the observed and retrieved soil temperatures is 2.0K. According to the evaluation of the sensitivity of retrieved component temperatures on fractional cover, the linear mixing model gives more accurate retrieval accuracies for both soil and vegetation temperatures under intermediate fractional cover conditions.

1. Introduction

Multi-angular TIR remote sensing data are considered capable of reflecting sub-pixel structure as well as component temperatures and provides a new information source in terrestrial energy balance studies [1-4]. Several radiative models have been established to account for this angular behavior [5-10]. Extensive ground-based multi-angular TIR measurements and the laboratory experiments have been carried out for theoretical research purposes [11-16]. Using multi-angular observations and physics-based models, the retrieval of component temperatures became possible [3, 17-19].

However, a lack of good-quality remote sensing data in suitable scale and angular setting is still the major obstacle in the applications of component temperatures retrieval [2, 20]. The most previous studies resorted to inversion of the physical thermal model to retrieve the component temperatures, which is usually time consuming and difficult to apply to satellite image data. The simple linear

*Corresponding author. Email: li.jia@wur.nl

mixing model is a practical algorithm using the multi-angular data obtained from few significant and independent angular measurements, such as AATSR (Advanced Along Track Scanning Radiometer) , and it provides the possibility of retrieving the wide range component temperatures from satellite data. However, the lack of the component temperature measurements at suitable spatial resolution makes the evaluation of retrieval results unfeasible. Aiming at evaluating the simple linear mixing model and its retrieval of component temperatures, a ground-based experiment using the thermal camera for multi-angular TIR measurements was operated in field in the Heihe River basin during the Hi-WATER (Heihe watershed Allied Telimetry Experimental Research) experimental campaign [21].

2. Data

This experiment was carried out during the Hi-WATER experimental campaign between July and August in 2012 in Zhangye, northwestern China, dominated by farmland. The intensive TIR measurements using thermal camera and radiometers were carried out over vegetable and orchard fields during the Hi-WATER campaign. The vegetable plots were dominated by pepper, celery and cauliflower. The orchard plot was dominated by apple trees. The following TIR data was collected: (1) multi-angular thermal images of the vegetation canopy and soil acquired by a thermal camera (Fluke Ti55FT) over the orchard canopy on August 27th(every 2 hours from 10:00am to 18:00 except 12:00am), the observing zenith angles were approximately set at 30° and slightly larger than 60°at a tower of 30 m height and captured thermal images have the dimension of about 10m x 10m; multi-angular data with the dimension of about 20cm x 20cm collected on July 31st from cauliflower and celery fields (in total three measurements over a day) at 0° and 50° at a ladder of 2.5 m height (2) single-angle images but with changing fraction of different components in the field-of-view (FOV) of the thermal camera by varying the snapshot areas over the soil-vegetation canopy of the vegetables, acquired by the thermal camera at the ladder. The thermal image also has the dimension of about 20cm x 20cm. Two sunny days' single angular thermal camera data was collected every hour on August 18th and 19th from pepper canopy. The thermal camera was calibrated with a blackbody at the end of the field campaign and the calibration results were used to correct the field experimental data.

3. Methodology

3.1. The linear mixing model

The linear mixing model of thermal infrared radiative transfer for heterogeneous soil-vegetation system developed by Jia (2004)[18] was used in this study. Ignoring the reflected atmosphere long wave radiance, the thermal infrared radiance of a soil-vegetation canopy can be simplified as a linear mixing of exitance of the soil and vegetation components weighted by their fraction of areas as below,

$$\mathrm{B}\big(T_b(\theta)\big) = F_c(\theta)\varepsilon_f(\theta)'B\big(\bar{T}_f\big) + \big(1 - F_c(\theta)\big)\varepsilon_s(\theta)'B(\bar{T}_s) \quad (1)$$

where B is the Planck function, $T_b(\theta)$ is the brightness temperature of a scene or a pixel, θ is the observing zenith angle , $F_c(\theta)$ is the fractional cover of vegetation in a scene or pixel, $\varepsilon_f(\theta)'$ is the effective emissivity of vegetation calculated by Eq. (2), $\bar{T}_f$ is the mean radiometric temperature of vegetation, $\big(1 - F_c(\theta)\big)$ is the fractional cover of soil, $\varepsilon_s(\theta)'$ is the effective soil emissivity calculated by Eq. (3), and $\bar{T}_s$ is the mean radiometric temperature of soil. Here, the effective emissivity of soil and vegetation are used considering the interaction between vegetation–soil and vegetation–vegetation[22]:

$$\varepsilon_s(\theta)' = \big\{1 + \big(1 - \varepsilon_f\big)(1 - P_h)F_c(\theta)[1 - F_c(\theta)]^{-1}\big\}\varepsilon_s \quad (2)$$

$$\varepsilon_f(\theta)' = \{1 + (1 - \varepsilon_s)(1 - P_h)[1 - F_c(\theta)][F_c(\theta)]^{-1}\}\varepsilon_f \quad (3)$$

where P_h is the hemispheric gap frequency, defined as $P_h = \frac{1}{\pi}\int_{\frac{\pi}{2}}^{\frac{\pi}{2}}(1 - Fc(\theta))\,\mathrm{d}\theta$. In this paper, P_h is simply taken as the $(1 - Fc(\theta))$, ε_s is the soil emissivity, ε_f is the vegetation emissivity.

3.2. Evaluation approach

The evaluation of the linear mixing radiative transfer model includes two parts: evaluation of the linear mixing model and evaluation of the inversion of component temperatures. In the evaluation, a whole thermal camera image was treated as a pixel.

To evaluate the linear mixing model (Eq. (1)), the soil and vegetation component temperatures and fractional cover of each component must be known a priori. The thermal image was first classified into two categories, soil and vegetation, using temperature thresholds and further corrected using concurrent visible CCD photos. The fractional cover of each component was extracted from the thermal images based on the classification. The mean brightness temperatures of the soil and vegetation components, referred as observed brightness component temperatures $\bar{T}_{b\_f}$ and $\bar{T}_{b\_s}$, were obtained by averaging the temperatures of each one of the two classes in the thermal image by:

$$\mathrm{B}\big(T_b(\theta)\big) = \frac{1}{n}\sum_{i=1}^{n} B\big(T_i(\theta)\big) \tag{4}$$

where n is the number of the pixels of either soil or vegetation in the whole thermal camera scene, $T_i(\theta)$ is the brightness temperature of the pixel i classified as soil or vegetation in the scene.

Then the radiometric temperatures of the vegetation and soil, $T_{rad\_f}(\theta)$ and $T_{rad\_s}(\theta)$, was obtained from the $T_b(\theta)$ of vegetation and soil , $\bar{T}_{b\_f}$ and $\bar{T}_{b\_s}$, by the corrections for emissivities as:

$$B\big(T_b(\theta)\big) = \varepsilon_e(\theta)\mathrm{B}\big(T_{rad}(\theta)\big) \tag{5}$$

where $\varepsilon_e(\theta)$ is the effective component emissivity, respectively $\varepsilon_s(\theta)'$ and $\varepsilon_f(\theta)'$, which were calculated by Eq. (2) and Eq. (3) using measured emissivities of foliage and soil: ε_f = 0.973 and ε_s = 0.957(personal communication with Dr. Mu who did the measurements of the component temperatures). $\mathrm{T_{rad}}(\theta)$ is the observed radiometric temperature of components, respectively $T_{rad\_f}(\theta)$ and $T_{rad\_s}(\theta)$, which will be written as $T_{f\_observed}(\theta)$ and $T_{s\_observed}(\theta)$.

Finally to evaluate the two-component linear mixing model, mean component radiometric temperatures, component fractional covers and effective component emissivities were applied in Eq. (1) to obtain the model simulated brightness temperature $T_b(\theta)$ of the whole scene observed by the thermal camera. The model simulated brightness temperature $T_b(\theta)$ was compared with the observed brightness temperature $T_{b\_observed}(\theta)$, the latter was calculated by Eq. (4) by taking n as the number of pixels in the whole thermal camera scene and $T_i(\theta)$ as the brightness temperature of the pixel i in the scene.

For evaluation of the model inversion, the $T_{b\_observed}(\theta)$ and $F_c(\theta)$ at two view angles or from a pair of images which were observed at single-angle but with changing fraction of different components in the field-of-view (FOV) of the thermal camera by varying the snapshot areas were obtained and taken as input in Eq. (1) to solve the two equations (each at one view angle) for the soil and vegetation temperatures simultaneously, i.e. $T_{f\_retrieved}$ and $T_{s\_retrieved}$, respectively. For the two single-angle images in the pair, the image with the lower fractional cover was taken as the image as if it is observed at nadir view together with the other one in the pair as off-nadir view to compose artificially the two view angle observations. The retrieved component temperatures are then compared with the observed component temperatures $T_{f\_observed}(\theta)$ and $T_{s\_observed}(\theta)$. Besides, the Sd (standard deviation) of the observed temperatures also was used to evaluate the retrieved component temperatures.

4. Results

4.1. Evaluation of the linear mixing model

Figure 1 shows the scattering plot of comparison between the model simulated brightness temperature $T_b(\theta)$ from Eq. (1) using the approach described in Section 3.2 and the observed brightness temperature $T_{b\_observed}(\theta)$ using the thermal camera scenes taken over the vegetable and orchard plots.

The simulated brightness temperatures by the linear mixing model have good agreement with the observed brightness temperatures with the RMSE as 0.2K. The results also indicate that the mean

temperatures of soil and of vegetation derived from the thermal camera scenes are of good representative of the wide range of temperatures of soil and vegetation elements over a mixed land target, to be used in the linear mixing model.

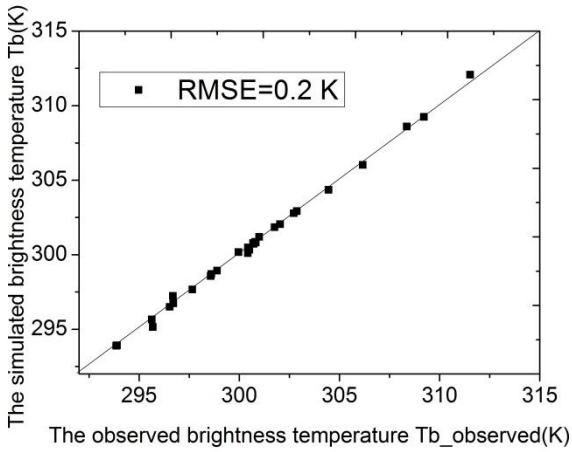

Figure 1. Comparison between simulated brightness temperature from the linear mixing model and the observed brightness temperature over vegetable and orchard canopies.

4.2. Results of inversion of the mixing model

The retrieved component temperatures from inversion of the linear mixing model Eq. (1) were compared with the reference mean components temperatures extracted from the thermal camera images (see Section 2) using the method given in Section 3.2. It is found that the component temperatures extracted from two images taken from two different angles (or from each one of the pair images) are quite close to each other, so the mean temperatures of components from two different images, $\bar{T}_f$ and $\bar{T}_s$, were taken as reference component temperatures.

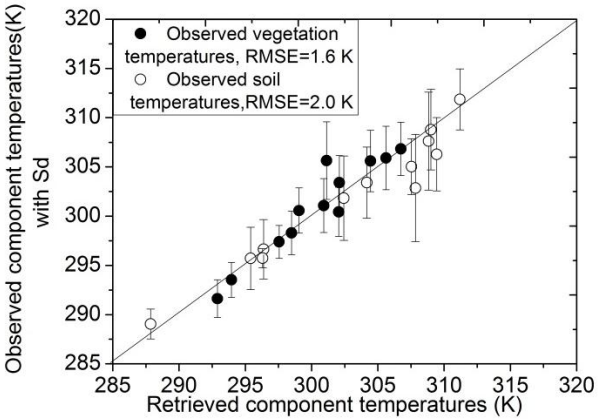

Figure 2. Comparison of the retrieved soil and vegetation temperatures with the observations extracted from the thermal camera images over vegetable and orchard canopies.

The RMSE between the model retrieved vegetation temperatures and the observed vegetation temperatures is 1.6K, and the RMSE for soil temperature comparison is 2.0K as shown in Fig. 2. The standard deviations of the extracted mean component temperatures are also given in Fig.2 indicating the range of the thermal properties of the two components captured by the thermal camera. Most retrieved component temperatures all stay within the range between$(\bar{T}_f \pm S_d)$ and $(\bar{T}_s \pm S_d)$ (Fig.2). This implies that the linear mixing model is reliable for retrieving component temperatures.

As discussed by Li et al[22], the inversion of the linear mixing model is sensitive to the accuracy of fractional vegetation cover, particularly to the difference of fractional vegetation cover between the nadir and the forward view angles. It was proved that the smaller the values of forward effective fractional cover ($F_{forward}$) (or nadir fractional cover (F_{nadir})) are, the larger are errors of T_f due to the errors of F_{nadir} (or $F_{forward}$), vice versa for the T_s in correspondence to fractional cover of soil [22, 23]. To evaluate the sensitivity of the retrieved component temperatures on the fractional cover, the extracted mean component temperatures from the thermal camera images (following the procedure in Section 3.2) were taken as the observed component temperatures. The absolute errors in the retrieved component temperatures are calculated as the absolute difference between the retrievaed component temperatures and the ones observed. Fig. 3 is the plot of the variation of the absolute errors in the retrieved component temperatures with the fractional cover (for multi-angular thermal images, the Fc(nadir) was from the image observed at nadir view; for single-angle images with changing fraction of different components, Fc(nadir) is taken from the image with the lower fractional cover of the pair images). Actually, the retrieval accuracy was influenced by many combined reasons, so the overall trend between the retrieval error sensitivity and fractional cover was not so obvious (Fig. 3). However, one may still see some useful hints from Fig. 3: when the nadir fractional cover was smaller than 0.5, the errors in the retrieved vegetation temperature (solid points) were larger than the error in the retrieved soil temperature (hollow points). At larger fractional vegetation cover, the errors in the retrieved soil temperatures were larger than the retrieved vegetation temperatures. One may conclude, based on the present study, that the linear mixing model gives more accurate retrieval accuracies for both soil and vegetation temperatures under intermediate fractional cover conditions.

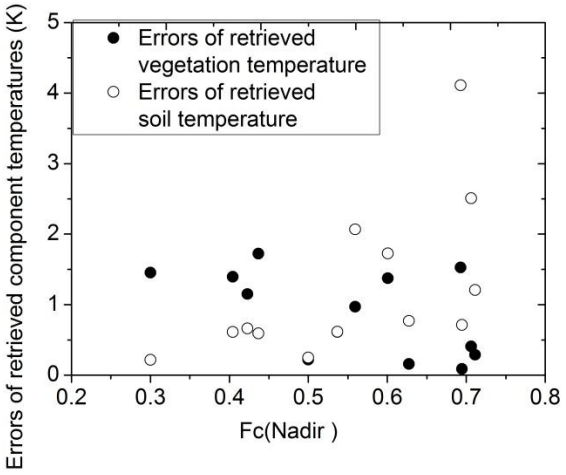

Figure 3. Errors in the retrieved component temperatures under different fractional vegetation cover over vegetable and orchard canopies.

5. Conclusions

This paper focused on linear mixing model validation by experimental data collected using thermal camera over vegetable and orchard fields. The preliminary results show that the linear mixing model is reliable and correct. For evaluation of the linear mixing model, the RMSE is 0.2 K between the observed brightness temperatures and the modelled brightness temperatures, which indicates that the linear mixing model works well under most conditions. The RMSE between the model retrieved vegetation temperatures and the observed vegetation temperatures is 1.6K, correspondingly, the RMSE between the model retrieved soil temperatures and the observed soil temperatures is 2.0K. Through the evaluation of the sensitivity of the retrieved component temperatures on the fractional cover, it was proved that the linear mixing model gives more accurate retrieval accuracies for both soil and vegetation temperatures under intermediate fractional cover conditions. As a preliminary

conclusion, this experimental study approves that the linear mixing radiative transfer model is a practical model for retrieving component temperatures with acceptable accuracy.

Acknowledgement: This work has been jointly supported by: the strategic research program KBIV 'Sustainable spatial development of ecosystems, landscapes, seas and region' funded by the Dutch Ministry of Economic Affairs and carried out by Wageningen UR, the EU-FP7 project CEOP-AEGIS (Grant nr. 212921) (http://ceop-aegis.org) and the "Chinese Academy of Sciences Visiting Professorships for Senior International Scientists".

References

[1] Menenti M, Jia L, and Li Z L 2008. *Advances in Land Remote Sensing:* **System**: p. 51-93.
[2] Liu Q, Yan C, Xiao Q, Yan G and Fang L 2011. *Int. J. Appl. Earth Obs. Geoinf.*, **17**, 66-75.
[3] François C 2002. *Remote Sens Environ*, **80**(1): p. 122-33.
[4] Djepa V, Menenti M, and Vaughan R 2002. *Adv Space Res*, **30**(11): p. 2529-33.
[5] Kimes D 1983. *Appl Opt*, **22**(9): p. 1364-72.
[6] Francois C, Ottlé C, and Prévot L 1997. *Int J Remote Sens*, **18**(12): p. 2587-621.
[7] Otterman J, Brakke T, and Susskind J 1992. *Boundary Layer Meteorol.*, **61**(1): p. 81-97.
[8] Chen L, Liu Q, Fan W, Li X, Xiao Q, Yan G and Tian G 2002. *Sci. China, Ser. D Earth Sci.*, **45**(12): p. 1087-98.
[9] Lagouarde J, Kerr Y, and Brunet Y 1995. *Agr. Forest Meteorol.*, **77**(3-4): p. 167-90.
[10] Kimes D, Holben B, TUCKER C J and Newcomb W 1984. *Int J Remote Sens*, **5**(6): p. 887-908.
[11] Labed J and M Stoll 1991. *Remote Sensing*, **12**(11): p. 2299-310.
[12] Liu Q H, Liu Q, Xin X Z, Deng R R, Tian G L, Chen L F, Wang J D, and Li X W 2001. IEEE
[13] Menenti M, Jia L, Li Z L, Djepa V, Wang J, Stoll M P, Su Z and Rast M 2001. *J Geophys Res*, **106**(D11): p. 11997-12,010.
[14] Sobrino J A et al 2005. //Proceedings of the ESA WPP-250: SPARC final workshop. 2005: 4-5
[15] Kimes D, Newcomb W, Schutt J, Pinter Jr P and Jackson R 1984. *Remote Sensing*, **5**(2): p. 263-77.
[16] Kimes D, Newcomb W., Tucker C J, Zonneveld I S, Van Wijngaarden W, De Leeuw J and Epema G F 1985. *Remote Sens Environ*, **18**(1): p. 1-19.
[17] Wang J, Li X, Sun X and Liu Q 2000. *Sci. China, Ser. E: Technolog. Sci.*, **43**: p. 41-47.
[18] Jia L 2004.Modeling heat exchanges at the land-atmosphere interface using multi-angular thermal infrared measurements (PhD Dissertation).
[19] Timmermans J, Verhoef W, Van der Tol C and Su Z 2009. *Hydrol Earth Syst Sci*, **13**(7): p. 1249.
[20] Jia L, Li Z, and Menenti M 2002. IEEE
[21] Li X et al 2013. Bull Am Meteorol Soc.
[22] Li Z, MP S, Zhang R, Jia L and Su Z 2001. *Sci. China, Ser. D Earth Sci.*, **44**(2): p. 97-111.
[23] Jia L, Li Z, Menenti M, Su Z, Verhoef W and Wan Z 2003. *Int. J. Remote Sens.*, **24**(23): p. 4739-60.